Since January 2020 Elsevier has created a COVID-19 resource centre with free information in English and Mandarin on the novel coronavirus COVID-19. The COVID-19 resource centre is hosted on Elsevier Connect, the company's public news and information website.

Colloids and Surfaces A: Physicochemical and Engineering Aspects 633 (2022) 127849

Contents lists available at ScienceDirect

Colloids and Surfaces A: Physicochemical and Engineering Aspects

journal homepage: www.elsevier.com/locate/colsurfa

Effect of hydroxychloroquine sulfate on the gelation behavior, water mobility and structure of gelatin

Hailin Wang [a,*], Wei Lu [b], Lijing Ke [a], Yi Wang [b], Jianwu Zhou [a], Pingfan Rao [a,*]

[a] Food Nutrition Science Centre, School of Food Science and Biotechnology, Zhejiang Gongshang University, 1st Lab Building, #149 Jiaogong Road, Xihu District, Hangzhou 310012, Zhejiang, China

[b] Department of Food Science and Engineering, School of Agriculture and Biology, Shanghai Jiao Tong University, Shanghai, China

GRAPHICAL ABSTRACT

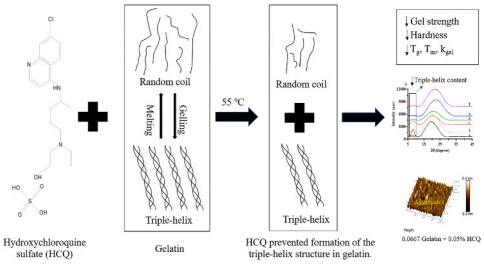

ARTICLE INFO

Keywords:
Gelatin
Hydroxychloroquine sulfate (HCQ)
Gelation behavior
Structure
Interaction

ABSTRACT

Hydroxychloroquine sulfate (HCQ) is a well-established antimalarial drug that has received considerable attention during the COVID-19 associated pneumonia epidemic. Gelatin is a multifunctional biomacromolecule with pharmaceutical applications and can be used to deliver HCQ. The effect of HCQ on the gelation behaviors, water mobility, and structure of gelatin was investigated to understand the interaction between the drug and its delivery carrier. The gel strength, hardness, gelling (T_g) and melting (T_m) temperatures, gelation rate (k_{gel}), and water mobility of gelatin decreased with increasing amounts of HCQ. The addition of HCQ led to hydrogen bonding that interfered with triple helix formation in gelatin. Fourier transform infrared spectroscopy (FTIR) and X-ray diffractometer (XRD) analysis further confirmed that the interaction between HCQ and gelatin is primarily through hydrogen bonding. Atomic force microscopy (AFM) revealed that higher content of HCQ resulted in more and larger aggregates in gelatin. These results provide not only an important understanding of gelatin for drug delivery design but also a basis for the studying interactions between a drug and its delivery carrier.

1. Introduction

Hydroxychloroquine sulfate (HCQ) is a 4-aminoquinoline drug with antimalarial activity [1] that has been used to treat diseases, such as lupus erythematosus and rheumatoid arthritis [2,3]. Orally administered chloroquine and its derivative hydroxychloroquine result in adverse side effects, such as loss of appetite, nausea, and diarrhea. Similar adverse side effects occurred for the treatment of COVID-19

* Corresponding authors.
E-mail addresses: 504393065@qq.com (H. Wang), wei.lu@sjtu.edu.cn (W. Lu), lijingke@zjgsu.edu.cn (L. Ke), wangyi51@sjtu.edu.cn (Y. Wang), jianwuzhou@zjgsu.edu.cn (J. Zhou), pingfanrao@mail.zjgsu.edu.cn (P. Rao).

https://doi.org/10.1016/j.colsurfa.2021.127849
Received 27 September 2021; Received in revised form 28 October 2021; Accepted 30 October 2021
Available online 3 November 2021

associated pneumonia. Previous studies have shown that biocompatible and degradable biomacromolecules (e.g., dextran, gelatin, etc) can be used as delivery carriers for HCQ improve its efficacy and reduce its toxicity and side effects [4–6]. For example, Bajpai et al. [4] prepared gelatin nanoparticles using water/oil emulsion technology and added a glutaraldehyde crosslinking agent to carry hydroxychloroquine phosphate. The results showed that loading the hydroxychloroquine phosphate onto a carrier could reduce the side effects and lower the release rate of HCQ.

Gelatin is a natural, highly biocompatible, biodegradable, biomacromolecule, with low immunogenic potential, that has a long history of applications in the food, cosmeceuticals, pharmaceutical, and medical fields and has been recognized as a safe biomaterial by the Food and Drug Administration (FDA) of the United States [7,8]. The physical and chemical properties of gelatin, especially its crosslinking density, degradation kinetics, and gel properties, provide many possibilities for designing drug delivery carriers. Therefore, their (either alone or in support of any other polymer) application in the field of medicine is attracting increasing attention [9–11]. At present, research on the use of gelatin in the field of medicine is primarily focused on the encapsulation and targeted delivery of compounds, such as anticancer and miscellaneous drugs, proteins, and vaccines to improve the in vivo degradation kinetic parameters, improve therapeutic effects, and reduce toxicity and side effects [12–16]. However, research on how drugs and excipients interact with gelatin and alter their structure and properties in complex delivery systems is still limited. Therefore, to develop more pharmaceutical applications for gelatin, it is necessary to study the interaction between gelatin and drugs.

Herein, the effect of different contents of HCQ on the gel strength, texture, gelation temperature (T_g), melting temperature (T_m), gelation kinetics, and water distribution of gelatin is reported, along with changes in the gelatin structure and interaction mechanism between gelatin and HCQ.

2. Materials and methods

2.1. Materials and reagents

Gelatin from porcine skin (type A, 300 bloom) was purchased from Sigma Chemical Co. Ltd. (St. Louis, MO, USA). Hydroxychloroquine sulfate (HCQ) was purchased from Jinlan Pharmaceutical Technology Development Co., Ltd. with a purity of 99.55%. Potassium bromide (KBr) was purchased from Shanghai Shanyue Scientific Instrument Co., Ltd. Ultrapure water used in the experiment was prepared by a Millipore Milli-Q system (Millipore, Bedford, MA, USA).

2.2. Preparation of samples

Ultrapure water (30 mL) was warmed in a 55 ℃ water bath for 10 min and different amounts of HCQ were added to prepare aqueous solutions containing 0%, 1%, 3%, 5%, 7% and 9% (w/v) HCQ. Gelatin was then dissolved in the HCQ solution at 55 ℃ to obtain samples with a mass fraction of 6.67% gelatin having different contents of HCQ (w/v).

2.3. Determination of gel strength

The gel strength of the samples was determined according to the method described by Kaewruang et al. [17]. The samples prepared in Section 2.2. were allowed to sit for 16–18 h at 4 ℃, and the gel strength was measured using a TA.XT Plus texture analyzer (Stable Micro Systems, Surrey, UK). The test mode used was pre-test speed: 1 mm/s; test speed: 0.5 mm/s; post-test speed: 0.5 mm/s; target mode: distance; distance: 8 mm (the height of gel was 25 mm); trigger type: auto (force); trigger force: 0.05 N.

2.4. Texture profile analysis (TPA)

TPA was performed according to the method proposed by Kaewruang et al. [17]. The samples prepared in Section 2.2. were allowed to sit at 4 ℃ for 16–18 h, and TPA was performed using a TA.XT Plus texture analyzer (Stable Micro Systems, Surrey, UK). The test mode used was pre-test speed: 1 mm/s; test speed: 0.5 mm/s; post-test speed: 0.5 mm/s; target mode: distance; compression: 30%; trigger type: auto (force); trigger force: 0.05 N, tare mode: auto; and advanced options: on.

2.5. Determination of gelling and melting temperatures

The gelling (T_g) and melting (T_m) temperatures of the samples prepared in Section 2.2. were measured using a rheometer (MCR 302, Anton Paar, Germany) according to the method of Liu et al. [18], with slight modifications. A small vibration shear mode, 0.5% strain, and 1 Hz frequency were used for testing. All the measurements were carried out from 40 to 5 ℃ and 5–40 ℃, with cooling and heating rates of 0.5 ℃/min. The store modulus (G′), loss modulus (G″), and phase angle (tan δ) were recorded. The T_g and T_m were determined from the cross-over point of G′ and G″ during cooling and heating, respectively.

2.6. Gelation kinetics

The gelation kinetics of the samples prepared as given in Section 2.2. were determined using a rheometer (MCR 302, Anton Paar, Germany), with slight modifications to the previous method [19]. All the samples were cooled from 25 to 4 ℃ at a rate of 1 ℃/min and then maintained at 4 ℃. The G′ and G″ values of the samples were recorded for 3 h at a constant strain of 0.5% and frequency of 1 Hz. The evolution of G′ over a fixed time period of gelation was fitted to the following logarithmic equation:

$$G_t = k_{gel} \ln(t_{gel}) + C$$

where G_t is the value of G′ at a given time (min), C is a constant, k_{gel} is the gelation rate, and t_{gel} is the gelation time. The value of G′ of the sample without HCQ was used as the model to obtain the target G′ (G'_{ref}) after 3 h cooling and gelling at 4 ℃. The time (t_{model}) required for a gelling system to reach G'_{ref} with different HCQ contents was calculated using the following equation:

$$t_{model} = e^{(G'ref - C)}/k_{gel}$$

2.7. Fourier transform infrared spectroscopy (FTIR)

The samples prepared in Section 2.2. were freeze-dried (2 mg), mixed with KBr powder, ground, and pressed into pellets. The FTIR spectra of the samples were recorded using a FTIR spectrophotometer (Nicolet 380, Thermo Fisher Scientific, USA) in the wavenumber range of 600 – 4000 cm^{-1}.

2.8. Low-field nuclear magnetic resonance (LF NMR)

A 3 mL aliquot of the sample solution prepared in Section 2.2. was withdraw, placed in a 15 mm diameter NMR tube, and maintained at 4 ℃ for 12 h. The water mobility and distribution of each sample was determined using LF NMR (NMI20-015 V-I, Niumag (Shanghai) Electric Corporation, China). The parameters used were as follows: CPMG pulse sequence, duration between successive scans is 6000 ms, number of scan is 4, spectral width is 250 kHz, time of echoes is 0.5 ms, and number of echoes is 15,000.

2.9. X-ray diffraction measurement (XRD)

The samples prepared in Section 2.2. were freeze-dried (2 mg) and analyzed using a X-ray diffractometer (Ultima IV X, Rigaku, Japan) at 2θ values ranging from 5° to 45° at a rate of 2°/min. The voltage was 40 kV, and electric current was 40 mA.

2.10. Atomic force microscopy (AFM)

The sample prepared in Section 2.2. were diluted 100-fold with deionized water, and the nanostructure of the samples were characterized by atomic force microscopy (Multimode 8, Bruker, Germany) according to the method described by Huang et al. [19], with some modifications. In short, 10 μL of each sample was dripped on the freshly-cleaved mica surface and dried for more than 12 h in a desiccator. The imaging was conducted in a tapping mode to characterize the nanostructure in air at ambient temperature.

2.11. Statistical analysis

All the experiments were conducted in duplicate and the data were expressed as means ± standard deviation (SD). Statistical data were analyzed using GraphPad Prism 8 (GraphPad Software) and SPSS software version 26 (IBM software). One-way analyses of variance (ANOVA) were carried out and mean comparisons were run by Duncan's Multiple Range Tests ($p < 0.05$).

3. Results and discussion

3.1. Gel strength analysis

The effect of different HCQ contents on the gel strength of gelatin is shown in Fig. 1A and Table S1. The gel strength of the gelatin decreased significantly with the increase in HCQ content ($p < 0.05$), from a gel strength of 302.3 g (control) to a gel strength of 145.2 g (9% HCQ). The gel strength of gelatin depends on the hydrogen bonds formed between the gelatin hydroxyl groups and free water as well as hydrogen bonds formed between the interchain carbonyl groups [17,20,21]. HCQ reduces the gel strength of gelatin, as it competes with the gelatin hydroxyl groups for water molecules, thereby weakening the hydrogen bonding between the gelatin hydroxyl groups and free water. HCQ also destroys the intramolecular hydrogen bonds within gelatin, thus reducing self-aggregation of the gelatin molecules and consequently gel strength.

3.2. TPA analysis

The effect of different contents of HCQ on the gelatin hardness is shown in Fig. 1B and Table S1. The gelatin hardness decreased with the increase in HCQ content ($p < 0.05$), from a hardness of 1127.6 g (control) to a hardness of 741.6 g (9% HCQ), which was consistent with the gel strength results (Fig. 1A). The content of HCQ had no significant effect on the cohesiveness of the gelatin (Fig. 1C, $p > 0.05$), which is the gel's ability to maintain a complete network structure [22]. The gumminess of the gelatin, which is related to hardness, decreased with the increase in HCQ content (Fig. 1D, $p < 0.05$), consistent with the hardness results. The springiness of the gelatin increased significantly ($p < 0.05$) when it contained 3% HCQ, but there was no significant difference between the other HCQ contents (Fig. 1E, $p > 0.05$). The springiness is determined by the degree of breakage of the gel structure during the first TPA compression process, which can be used to indicate the "rubber" of the gel in the mouth [22]. The chewiness of the gelatin was also consistent with the hardness results, it decreased significantly with the increase in HCQ content (Fig. 1F, $p < 0.05$). Previous studies have shown that the hydrogen bonding within the gelatin systems and the size of gelatin molecular chains can affect the textural properties of gelatin [23]. Therefore, the effect of HCQ on the gelatin texture is probably due to the decrease in the intramolecular hydrogen bonding and length of the molecular chains of the gelatin in the system. These results are consistent with the gel strength analysis results.

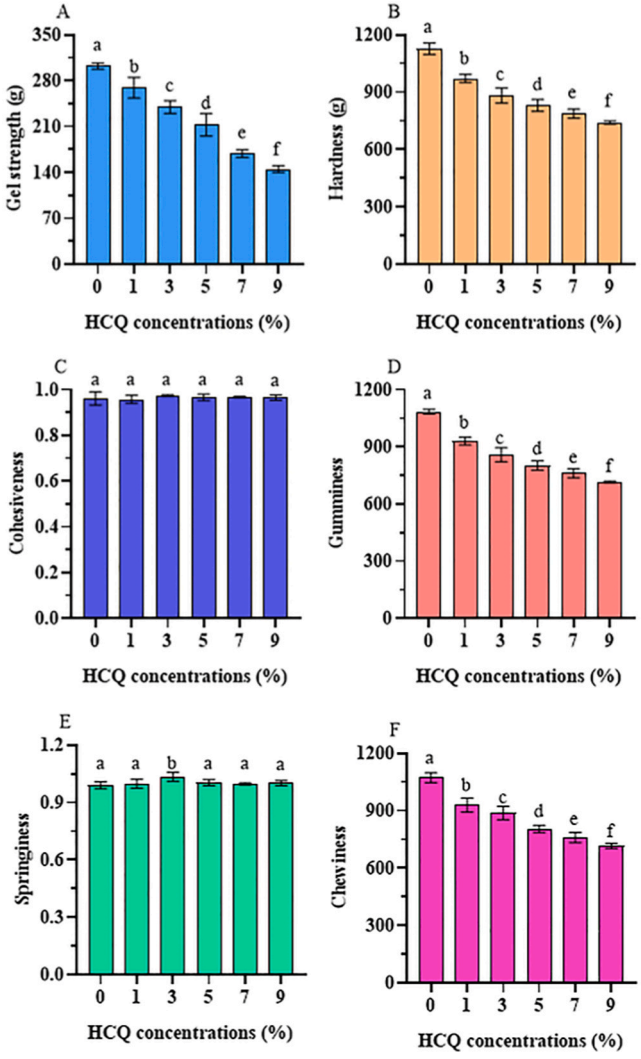

Fig. 1. Gel strength (A), hardness (B), cohesiveness (C), gumminess (D), springiness (E) and chewiness (F) of gelatin (6.67%, w/v) with different contents (0%, 1%, 3%, 5%, 7%, and 9%, w/v) of HCQ.

3.3. Gelling and melting temperature analysis

The storage (G′) and loss (G″) moduli of gelatins having different contents of HCQ are presented in Fig. 2A-B and Fig. S1. Gelatin samples with different HCQ contents behaved as liquids initially at 40 ℃, with G′ lower than G″, whereas G′ was higher than G″ for the gelatin without HCQ. The values of G′ and G″ sharply increased as the temperature gradually decreased, indicating the formation of the gel. The temperature at the cross-over point of the G′ and G″ values during cooling is defined as the gelling temperature (T_g). During the heating process, G′ was much larger than G″ at the initial temperature (5 ℃), which shows a solid behavior. The value of G′ and G″ both sharply decreased as the temperature continuously increased and finally G″ exceeded G′, which shows a liquid behavior. The temperature at the cross-over point of G′ and G″ during the heating process is defined as the melting temperature (T_m).

The T_g and T_m values of gelatin with different contents of HCQ are shown in Table 1. The T_g and T_m of the gelatins decreased as the HCQ content increased. The gelatin gels are formed by the transition of a

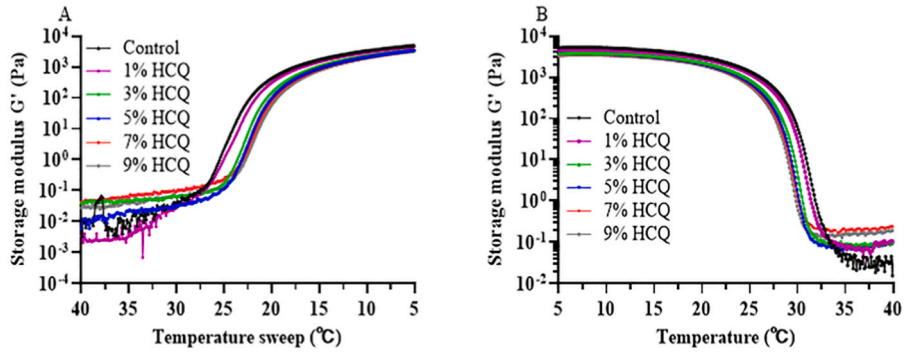

Fig. 2. Storage modulus (G′) of gelatin with different contents of HCQ upon cooling from 40 ℃ to 5 ℃ (A) and upon heating from 5 ℃ to 40 ℃ (B). Control: 6.67% gelatin (w/v); 1% HCQ, 3% HCQ, 5% HCQ, 7% HCQ, 9% HCQ (w/v): 6.67% gelatin prepared by the different contents of HCQ solutions.

Table 1
Gelling (T_g) and melting (T_m) temperature points, and parameters for the analogue function model used to fit the gelation profiles of gelatin with different contents of HCQ.

Samples	Control	1% HCQ	3% HCQ	5% HCQ	7% HCQ	9% HCQ
T_g (℃)	26.11 ± 0.17^{a}	25.40 ± 0.66^{ab}	24.06 ± 0.58^{b}	23.42 ± 0.16^{bc}	23.06 ± 0.66^{bc}	22.83 ± 0.33^{c}
T_m (℃)	32.01 ± 0.00^{a}	31.36 ± 0.41^{b}	30.37 ± 0.17^{c}	30.02 ± 0.17^{cd}	29.84 ± 0.08^{d}	29.61 ± 0.08^{d}

Values are mean ± SD. Values with different letter whithin the same column are significantly different ($p < 0.05$). Control: 6.67% gelatin (w/v); 1% HCQ, 3% HCQ, 5% HCQ, 7% HCQ, 9% HCQ (w/v): 6.67% gelatin prepared by the different contents of HCQ solutions.

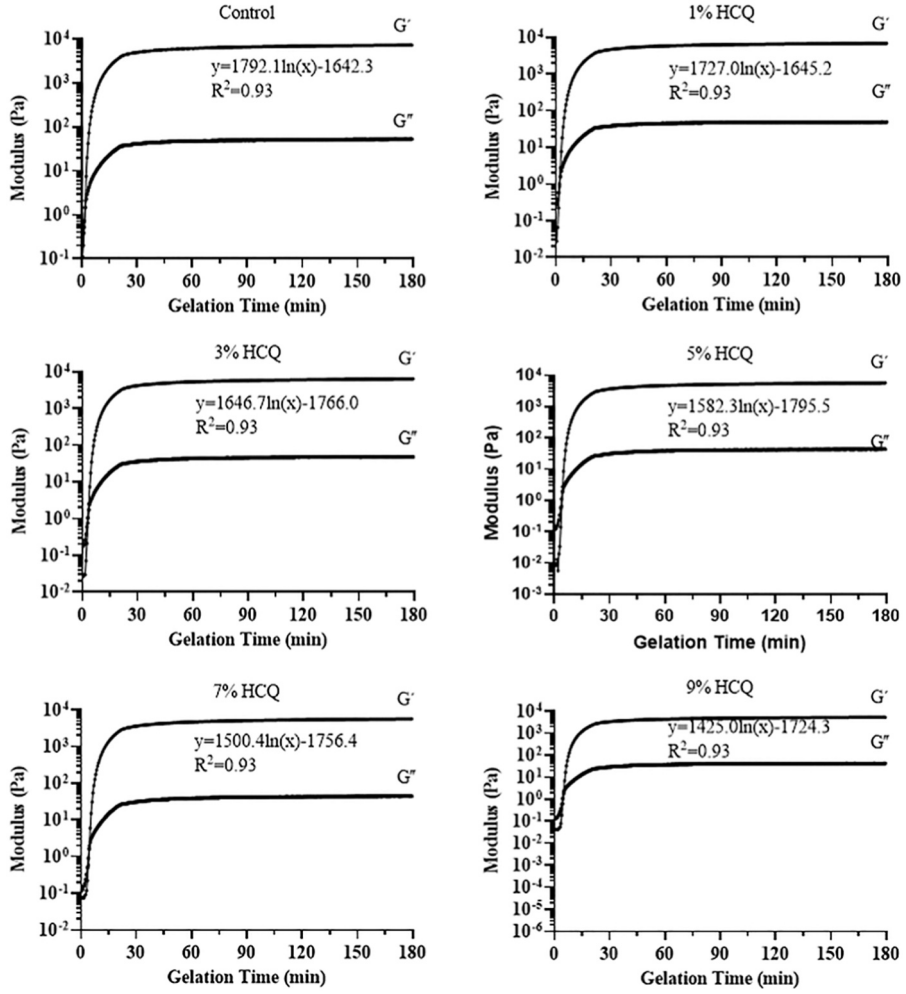

Fig. 3. Evolution of storage (G′) and loss (G) modulus during cooling and gelling of gelatin with different contents of HCQ. Control: 6.67% gelatin (w/v); 1% HCQ, 3% HCQ, 5% HCQ, 7% HCQ, 9% HCQ (w/v): 6.67% gelatin prepared by the different contents of HCQ solutions.

single-strand structure to a triple-helix via hydrogen bonding, van der Waals force, self-assembly, and ionic interaction [24,25]. Naftalin et al. [26] and Kuan et al. [27] suggested that changes in the T_g and T_m of gelatin in the presence of sugar were caused by the interaction between sugar molecules and gelatin through hydrogen bonds, and that the existence forms of the water molecules in the system, were differ from its normal involvement with sugars or gelatin individually. The decrease in T_g and T_m can be explained by HCQ breaking the hydrogen bonds between the gelatin molecular chains and weakening the hydrogen bonds between the gelatin hydroxyl groups and free water, thus preventing formation of the gel's triple helix structure.

3.4. Gelation kinetics

The formation kinetics and mechanical stability of the gelatin gels were evaluated by the changes in G′ and G″during cooling and gelling of the gelatin. The kinetics results of gelatins with different HCQ contents are shown in Fig. 3 and Table S2. The G″values were larger than the G′ values at the initial temperature (25 ℃). However, the value of G′ rapidly exceeded that of G″during the cooling process, suggesting gel formation. The value of G′ increased with time during the cooling process and when the gel was maintained at 4 ℃, but the rate of increase in the G′ value with time decreased in all samples after 30 min owing to the formation of the gel network. These results indicate that the gel strength of all the samples increased with time due to the formation of a helical structure at 4 ℃, consistent with the report by Huang et al. [19] and Renato et al. [28].

As seen in Table S2, k_{gel} was negatively correlated with the HCQ content. The same trend was observed for the time needed for the gelling system to reach the value of G'_{ref} from gelling the gelatin under the same conditions. The k_{gel} of gelatin decreased from 1792.1 without HCQ to 1727.0, 1646.7, 1582.3, 1500.4, and 1425.0 upon the addition of 1%, 3%, 5%, 7%, and 9% HCQ, respectively. Previous studies demonstrated that the k_{gel} of gelatin is related to the distance between the molecular chains and formation of hydrogen-bonded triple-helix junctions during gelation [19,24,29]. Therefore, the decrease in k_{gel} and increase in gelling time in the presence of HCQ further demonstrated that the typical hydrogen-bonded triple-helix junctions of gelatin that form during cooling were gradually disrupted by the addition of HCQ. HCQ prevented the gelatin chains from approaching each other during gelation, thereby reducing k_{gel}.

3.5. FTIR analysis

FTIR is based on biomolecular maps of various compounds, which primarily depends on their molecular structure and composition [30]. The FTIR spectra and locations and assignments of each peak for gelatins with different contents of HCQ are presented in Fig. 4 and Table S3. The locations and assignments of each peak were analyzed according to the method described by shurvell [31]. All the gelatin samples had a strong peak in the 3520 – 3320 cm^{-1} range, which is the N-H stretching vibration or O-H stretching vibration of the amide A band, indicating the existence of hydrogen bonds in the gelatin [32,33], HCQ peak was observed at 3389 cm^{-1}. Compared with amide A band of the control (3422 cm^{-1}), the corresponding peak for gelatins containing 1% or 3% HCQ shifted to a higher wavenumber (3422 and 3442 cm^{-1}, respectively), whereas the corresponding peak shifted to a lower wavenumber when HCQ was increased to 5%, 7%, or 9% (3405, 3385, and 3401 cm^{-1}, respectively). These changes indicate that the addition of HCQ can affect the hydrogen bonding in the gelatin system. In addition, when 7% or 9% HCQ was added, a small peak was observed at 3111 cm^{-1} that corresponded to a HCQ peak at 3102 cm^{-1}, which is the stretching vibration of an O-H group. The peaks in the 2990–2850 cm^{-1} range for all the gelatin samples are C-H antisymmetric and symmetric stretching vibrations of the amide B band. The peaks appear at different wavenumbers depending on the concentration of HCQ. The peak at

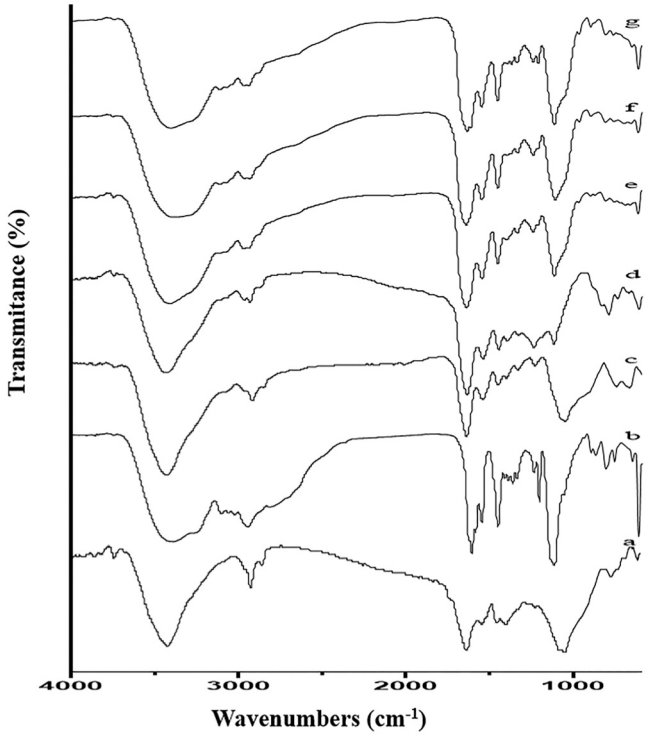

Fig. 4. FTIR spectra of gelatin with different contents of HCQ. (a), 6.67% gelatin (w/v); (b), HCQ; (c-g), 6.67% gelatin prepared by the content of 1%, 3%, 5%, 7%, 9% HCQ (w/v) solution, respectively.

1648–1638 cm^{-1} is the amide I band, which is the stretching vibration absorption peak of the C═O group and related to the secondary structure of proteins. This peak can be used to characterize the triple helix and irregular coil structure in gelatin [34]. The addition of HCQ makes the peak move to a higher wavenumber. A HCQ peak is at 1614 cm^{-1}. The amide II band (1470–1570 cm^{-1}) is also used to characterize changes in the secondary structure of gelatin [34], and the position of the amide II band shifted to a longer wave number depending on the content of HCQ added. Thus, based on the change in the peak positions of the amide I (1648 cm^{-1}) and amide II (1543 cm^{-1}) bands, the addition of HCQ changed the -N = CH- structure of gelatin, possibly by forming a new secondary amide bond, which affected the triple helix and irregular coil structure of gelatin. In addition, the effect of HCQ on the peak position of the amide III band was not noticeable, except when 1% HCQ was added the peak position moved to a lower wavenumber. In the fingerprint region, when 3%, 5%, 7% or 9% HCQ was added, an absorption peak appeared at 620 cm^{-1}, which corresponded to a C-O stretching vibration absorption peak. These peak shifts indicate that HCQ interacts with gelatin by influencing the formation of hydrogen bonds and the triple helix structures.

3.6. LF NMR analysis

The water content and distribution in gelatin influence the gelation properties and quality of the gelatin. LF NMR is a non-destructive and fast technique to measure the water content and distribution state in the food materials [35]. The relaxation time map can show three states of water: the bound water in a hydrate (T_{21}:0–10 ms), such as a water-protein conjugate, the immobile water in the material network structure (T_{22}:10–200 ms), and the free water in the system (T_{23}: 200–10,000 ms) [35,36]. The relaxation patterns of different contents of HCQ in the gelatin system are presented in Fig. 5 and Fig. S2, and the relaxation times and related peak area for all the samples is shown in Table S4.

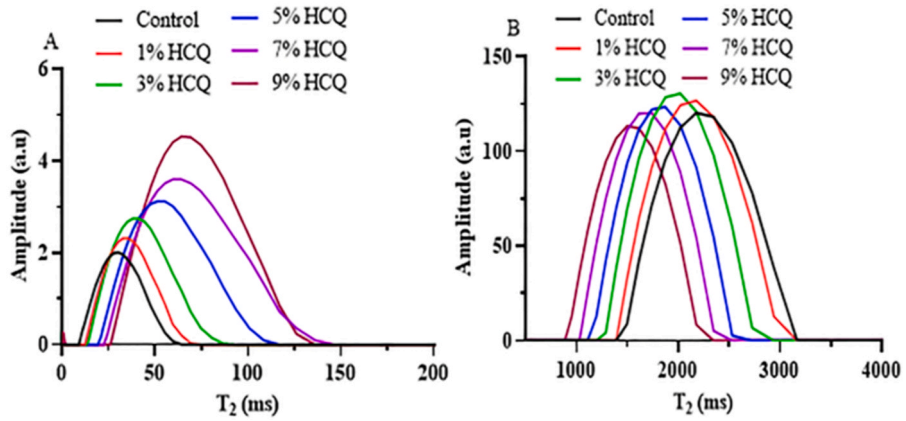

Fig. 5. The relaxation time curves of gelatin with different contents of HCQ. (A), Immobile water; (B), free water. Control: 6.67% gelatin (w/v); 1% HCQ, 3% HCQ, 5% HCQ, 7% HCQ, 9% HCQ (w/v): 6.67% gelatin prepared by the different contents of HCQ solutions.

All samples showed relaxation peaks in the ranges of 8–150 ms (T_{22}) and 850–3200 ms (T_{23}), while the samples containing 9% HCQ also had a weak relaxation peak in the range of 0–2.378 ms (T_{21}), although the peak area ratio of water bound in a hydrate (S_{21}%) was only 0.55%. Compared with the gelatin sample without HCQ, the relaxation time T_{22} increased in gelatin sample with 1% HCQ, but the ratio of T_{23} and the corresponding peak areas of the immobile water (S_{22}%) and free water (S_{23}%) almost unchanged. This may be because 1% HCQ only reduced the binding capacity of gelatin to the hydrogen protons of water, but had no influence on the ratio of immobile water to free water. When 3%, 5%, or 7% HCQ was added, the relaxation time T_{22} increased with the increase in HCQ content, whereas T_{23} decreased with the increase in HCQ content. However, when 9% HCQ was added, the relaxation times T_{22} and T_{23} were lower than those of the 7% HCQ sample. These results show that the binding ability of gelatin to the hydrogen protons of water was reduced by the adding HCQ. The corresponding peak area ratios had opposite trends: S_{22}% increased with the increase in HCQ content and S_{23}% decreased with the increase in HCQ content. This may be because the addition of HCQ to the gelatin systems can destroy the hydrogen bonds between the gelatin molecular chains, thus reducing the availability of hydrogen bonds that are required for formation of the gelatin triple helix structure and hindering the formation of the gelatin triple helix structure. This in turn reduces the size of the gelatin molecular chains and increases the content of small molecules in the system, thus exposing more hydrophilic groups that can combine with free water.

3.7. XRD analysis

XRD can be used to determine the crystallinity of the carrier materials (such as alginate, pectin, and gelatin) and biological complexes [32]. The XRD patterns of HCQ and gelatins having different contents of HCQ are shown in Fig. 6A and B. The gelatin without HCQ has a diffraction peak at $2\theta = 8.12°$ and a wider diffraction peak at $2\theta = 19.59°$, which indicates that gelatin is a semi-crystalline substance, and is consistent with the report by Liu et al. [34]. Compared with gelatin, HCQ has stronger crystallinity, with sharp and obvious crystallization peaks at $2\theta = 8.6°$, $10.8°$, $13.3°$, $17.0°$, $19.9°$, $21.8°$, $23.9°$, $26.7°$ and $28.9°$. When the gelatin contained HCQ, the diffraction peak intensity at $2\theta = 8.12°$ decreased and the peak shape widened with the increase in HCQ content. When the content of HCQ increased to 5%, 7% or 9%, there was only a weak diffraction peak near $2\theta = 8.12°$. These results may be in term of the existing interactions of gelatin surface with HCQ. Similar results were reported by García-Guzmán et al. [37]. The intensity of the diffraction peak at $2\theta = 19.59°$ first decreased and then increased with an increase in the HCQ content, and the peak shape widened with the increase in HCQ content. This indicates that the addition of HCQ can change the crystallization characteristics of gelatin.

Furthermore, the diffraction peak of gelatin at $2\theta = 8.12°$ is an indicator of the triple helix structure in gelatin, and its intensity corresponds to the triple helix content [38,39]. As seen in Fig. 6A, the intensity of the diffraction peak at $2\theta = 8.12°$ decreased with increasing HCQ content, which suggested that the triple helix content in gelatin decreased. Because the formation of the triple helix structure in gelatin involves hydrogen bonding [34,40], the decrease in the intensity of the diffraction peak at $2\theta = 8.12°$ indicates that the addition of HCQ can inhibit the formation of the triple helix structure of gelatin by disrupting hydrogen bonding, which further affects the gelation behaviors and structure of the gelatin. In addition, the XRD results further indicate that

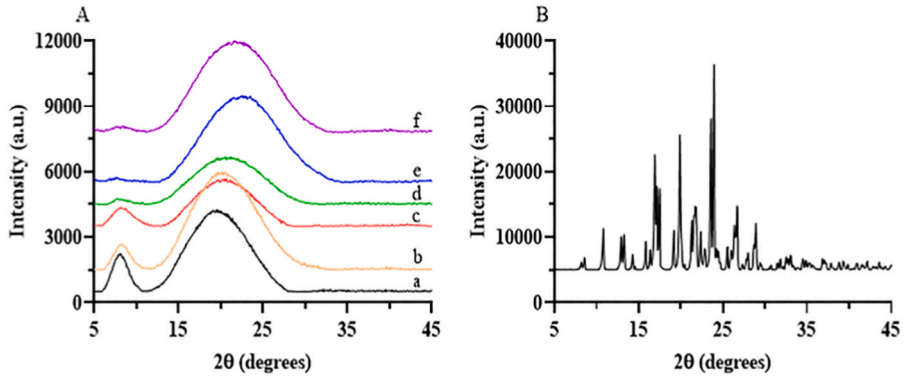

Fig. 6. XRD pattern of gelatin with different contents of HCQ (A) and HCQ (B). (a), 6.67% gelatin (w/v); (b), HCQ; (c-g), 6.67% gelatin prepared by the content of 1%, 3%, 5%, 7%, and 9% HCQ (w/v) solutions, respectively.

adding HCQ could reduce the gel strength and hardness of gelatin, primarily because the addition of HCQ hindered the triple helix structure of the gelatin molecules [41]. However, when the HCQ content increased to 5%, the gel strength and hardness continued to decrease, probably owing to the addition of excessive HCQ.

3.8. AFM analysis

The underlying mechanism of the changes in gelatin properties can be analyzed by AFM [25]. According to previous studies, the nanostructure of gelatin was related to the extraction method, concentration,

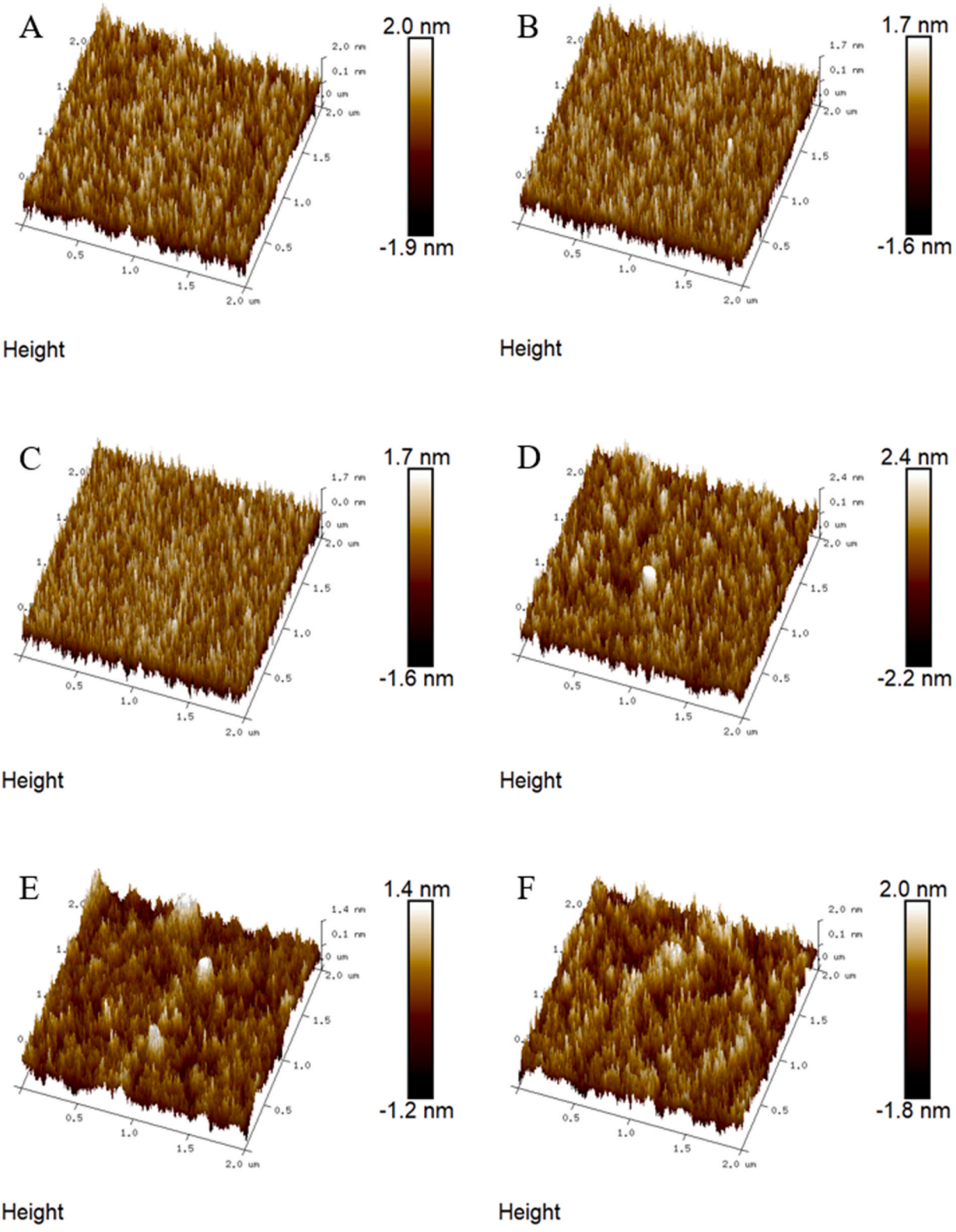

Fig. 7. Nanostructure of gelatin solution at 0.0667% (w/v). A, B, C, D, E, F: gelatin contained various HCQ content (0%, 0.01%, 0.03%, 0.05%, 0.07%, and 0.09%), respectively.

modification method and experimentation [19,25,42]. Yang and Wang [42] reported that gelatins with high concentrations (1–6.67%) exhibited fibril nanostructure while most of the spherical structure for the low concentration gelatin (less than 1%). Huang et al. [19] found that longer time of phosphorylation led to looser gel network with more aggregation. However, limited studies used AFM to investigate the interaction between gelatin and drugs. Therefore, the effect of HCQ on the gelatin nanostructure was analyzed using AFM in the current study (Fig. 7).

As shown in Fig. 7A, the sample without HCQ contained some spherical aggregates. There was no significant difference in the nanostructure of the gelatin containing 0.01% and 0.03% HCQ. It was found that the mean surface roughness parameters of mean roughness (Ra) were decreased from 0.435 (control) to 0.379 (0.01% HCQ) and 0.368 (0.03% HCQ). However, larger aggregates on the surface were also noticed in the gelatin sample with 0.05% HCQ, which were previously not observed in the samples containing 0%, 0.01% and 0.03% HCQ, and the Ra increased to 0.499. On increasing HCQ content further, smaller but more aggregates could be found on the sample in the presence of 0.07% and 0.09% HCQ, also the Ra was 0.270 (0.07% HCQ) and 0.417 (0.09% HCQ), respectively. Furthermore, the conglomerate was also observed in the presence of 0.07% and 0.09% HCQ of gelatin sample. Farris et al. [43] reported that gelatin molecules could assemble into aggregates containing short segments. Huang et al. [25] found that the gelatin can form aggregates strongly via hydrogen bonds and electrostatic interaction. Therefore, the changes in the gelatin nanostructure with different content of HCQ might be attributed to the hydrogen bonding and the electrostatic repulsion interaction between gelatin and HCQ in the system.

4. Conclusion

The addition of HCQ decreased the gel strength, hardness, T_g, T_m, k_{gel}, and water mobility of gelatin by destroying the hydrogen bonding necessary for the formation of triple-helix junctions of gelatin during gelation. FTIR and XRD analyses further confirmed that the interaction between HCQ and gelatin primarily prevents the formation of the hydrogen-bonded triple-helix junctions. AFM revealed that higher content of HCQ (0.05%−0.09%) produced more and larger aggregates. These results can provide a better understanding of the effects of drugs on the gelation behaviors and structure of gelatin, which is beneficial for developing more applications of gelatin in the pharmaceutical industry. Moreover, this study can provide a reference for preparing HCQ-loaded gelatin to decrease the adverse effects of HCQ on the human body and also provide a basis for further studies on the interaction between a drug and its delivery carrier.

CRediT authorship contribution statement

Hailin Wang: Methodology, Validation, Formal analysis, Investigation, Data curation, Writing – original draft, Visualization. **Wei Lu:** Methodology, Data curation, Supervision. **Lijing Ke:** Methodology, Supervision. **Yi Wang:** Investigation. **Jianwu Zhou:** Supervision. **Pingfan Rao:** Conceptualization, Methodology, Validation, Resources, Writing-review & editing, Visualization, Supervision, Funding acquisition.

Declaration of Competing Interest

The authors declare that they have no known competing financial interests or personal relationships that could have appeared to influence the work reported in this paper.

Acknowledgments

This work was supported by the National Key Research and Development Plan of China (2016YFD0400202).

Appendix A. Supporting information

Supplementary data associated with this article can be found in the online version at doi:10.1016/j.colsurfa.2021.127849.

References

[1] T. Dongala, N.K. Katari, S.K. Ettaboina, A. Krishnan, M.M. Tambuwala, K. Dua, In vitro dissolution profile at different biological pH conditions of hydroxychloroquine sulfate tablets is available for the treatment of COVID-19, Front. Mol. Biosci. 7 (2021) 1–6, https://doi.org/10.3389/fmolb.2020.613393.
[2] N. Kasturi, Long-term continuation of chloroquine-induced retinal toxicity in rheumatoid arthritis despite drug cessation, Rheumatology 55 (2016) 766–768, https://doi.org/10.1093/rheumatology/kev400.
[3] K.P. Pryor, C. Xu, J.E. Collins, K.H. Costenbader, C.H. Feldman, Predictors of initial hydroxychloroquine receipt among medicaid beneficiaries with incident systemic lupus erythematosus, Arthritis Care Res. (2021) 0–2, https://doi.org/10.1002/acr.24572.
[4] A.K. Bajpai, J. Choubey, Design of gelatin nanoparticles as swelling controlled delivery system for chloroquine phosphate, J. Mater. Sci. Mater. Med. 17 (2006) 345–358, https://doi.org/10.1007/s10856-006-8235-9.
[5] G.A. Magalhães, E. Moura Neto, V.G. Sombra, A.R. Richter, C.M.W.S. Abreu, J.P. A. Feitosa, H.C.B. Paula, F.M. Goycoolea, R.C.M. de Paula, Chitosan/Sterculia striata polysaccharides nanocomplex as a potential chloroquine drug release device, Int. J. Biol. Macromol. 88 (2016) 244–253, https://doi.org/10.1016/j.ijbiomac.2016.03.070.
[6] A. Kashyap, R. Kaur, A. Baldi, U.K. Jain, R. Chandra, J. Madan, Chloroquine diphosphate bearing dextran nanoparticles augmented drug delivery and overwhelmed drug resistance in Plasmodium falciparum parasites, Int. J. Biol. Macromol. 114 (2018) 161–168, https://doi.org/10.1016/j.ijbiomac.2018.03.102.
[7] V. Sovilj, J. Milanovic, L. Petrovic, Influence of gelatin-sodium stearoyl lactylate interaction on the rheological properties of gelatin gels, Colloids Surf. A Physicochem. Eng. Asp. 417 (2013) 211–216, https://doi.org/10.1016/j.colsurfa.2012.11.009.
[8] J.T. Koivisto, C. Gering, J. Karvinen, R. Maria Cherian, B. Belay, J. Hyttinen, K. Aalto-Setälä, M. Kellomäki, J. Parraga, Mechanically biomimetic gelatin-gellan gum hydrogels for 3D culture of beating human cardiomyocytes, ACS Appl. Mater. Interfaces 11 (2019) 20589–20602, https://doi.org/10.1021/acsami.8b22343.
[9] M.S. Ali, K. Anjum, J.M. Khan, R.H. Khan, Kabir-ud-Din, Complexation behavior of gelatin with amphiphilic drug imipramine hydrochloride as studied by conductimetry, surface tensiometry and circular dichroism studies, Colloids Surf. B: Biointerfaces 82 (2011) 258–262, https://doi.org/10.1016/j.colsurfb.2010.08.043.
[10] Z.X. Meng, X.X. Xu, W. Zheng, H.M. Zhou, L. Li, Y.F. Zheng, X. Lou, Preparation and characterization of electrospun PLGA/gelatin nanofibers as a potential drug delivery system, Colloids Surf. B: Biointerfaces 84 (2011) 97–102, https://doi.org/10.1016/j.colsurfb.2010.12.022.
[11] M.F. Di Filippo, B. Albertini, L.S. Dolci, F. Bonvicini, A. Bigi, G.A. Gentilomi, N. Passerini, S. Panzavolta, Novel drug-loaded film forming patch based on gelatin and snail slime, Int. J. Pharm. 598 (2021), 120408, https://doi.org/10.1016/j.ijpharm.2021.120408.
[12] L.S. Dolci, B. Albertini, M.F. Di Filippo, F. Bonvicini, N. Passerini, S. Panzavolta, Development and in vitro evaluation of mucoadhesive gelatin films for the vaginal delivery of econazole, Int. J. Pharm. 591 (2020), 119979, https://doi.org/10.1016/j.ijpharm.2020.119979.
[13] M.F. Di Filippo, B. Albertini, L.S. Dolci, F. Bonvicini, A. Bigi, G.A. Gentilomi, N. Passerini, S. Panzavolta, Novel drug-loaded film forming patch based on gelatin and snail slime, Int. J. Pharm. 598 (2021), 120408, https://doi.org/10.1016/j.ijpharm.2021.120408.
[14] M.C. Echave, R. Hernáez-Moya, L. Iturriaga, J.L. Pedraz, R. Lakshminarayanan, A. Dolatshahi-Pirouz, N. Taebnia, G. Orive, Recent advances in gelatin-based therapeutics, Expert Opin. Biol. Ther. 19 (2019) 773–779, https://doi.org/10.1080/14712598.2019.1610383.
[15] E. Oh, J.E. Oh, J.W. Hong, Y.H. Chung, Y. Lee, K.D. Park, S. Kim, C.O. Yun, Optimized biodegradable polymeric reservoir-mediated local and sustained co-delivery of dendritic cells and oncolytic adenovirus co-expressing IL-12 and GM-CSF for cancer immunotherapy, J. Control. Release 259 (2017) 115–127, https://doi.org/10.1016/j.jconrel.2017.03.028.
[16] Y.W. Won, S.M. Yoon, K.S. Lim, Y.H. Kim, Self-assembled nanoparticles with dual effects of passive tumor targeting and cancer-selective anticancer effects, Adv. Funct. Mater. 22 (2012) 1199–1208, https://doi.org/10.1002/adfm.201101979.
[17] P. Kaewruang, S. Benjakul, T. Prodpran, A.B. Encarnacion, S. Nalinanon, Impact of divalent salts and bovine gelatin on gel properties of phosphorylated gelatin from the skin of unicorn leatherjacket, LWT - Food Sci. Technol. 55 (2014) 477–482, https://doi.org/10.1016/j.lwt.2013.10.033.
[18] P. Liu, H. Shen, Y. Zhi, J. Si, J. Shi, L. Guo, S.G. Shen, 3D bioprinting and in vitro study of bilayered membranous construct with human cells-laden alginate/gelatin composite hydrogels, Colloids Surf. B: Biointerfaces 181 (2019) 1026–1034, https://doi.org/10.1016/j.colsurfb.2019.06.069.
[19] T. Huang, Z. Tu, X. Shangguan, H. Wang, X. Sha, N. Bansal, Rheological behavior, emulsifying properties and structural characterization of phosphorylated fi sh gelatin, Food Chem. 246 (2018) 428–436, https://doi.org/10.1016/j.foodchem.2017.12.023.

[20] G. Zanaboni, A. Rossi, M.T. Onana, R.T. U, Stability and networks of hydrogen bonds of the collagen triple helical structure: influence of pH and chaotropic nature of three anions, Matrix Biol. 19 (2000) 511–520, https://doi.org/10.1016/S0945-053X(00)00096-2.
[21] R. Núñez-Flores, B. Giménez, F. Fernández-Martín, M.E. López-Caballero, M. P. Montero, M.C. Gómez-Guillén, Physical and functional characterization of active fish gelatin films incorporated with lignin, Food Hydrocoll. 30 (2013) 163–172, https://doi.org/10.1016/j.foodhyd.2012.05.017.
[22] M. Peleg, The instrumental texture profile analysis revisited Micha, J. Texture Stud. 50 (2019) 362–368, https://doi.org/10.1111/jtxs.12392.
[23] M. Nagarajan, S. Benjakul, T. Prodpran, P. Songtipya, Characteristics and functional properties of gelatin from splendid squid (Loligo formosana) skin as affected by extraction temperatures, Food Hydrocoll. 29 (2012) 389–397, https://doi.org/10.1016/j.foodhyd.2012.04.001.
[24] M.A. Da Silva, F. Bode, I. Grillo, C.A. Dreiss, Exploring the kinetics of gelation and final architecture of enzymatically cross-linked chitosan/gelatin gels, Biomacromolecules 16 (2015) 1401–1409, https://doi.org/10.1021/acs.biomac.5b00205.
[25] T. Huang, Z. cai Tu, H. Wang, X. Shangguan, L. Zhang, N. hai Zhang, N. Bansal, Pectin and enzyme complex modified fish scales gelatin: rheological behavior, gel properties and nanostructure, Carbohydr. Polym. 156 (2017) 294–302, https://doi.org/10.1016/j.carbpol.2016.09.040.
[26] R.J. Naftalin, M.C.R. Symons, The mechanism of sugar-dependent stabilisation of gelatin gels, BBA - Biomembr. 352 (1974) 173–178, https://doi.org/10.1016/0005-2736(74)90188-6.
[27] Y. Kuan, A. Mohammadi, N. Huda, F. Arif, A.A. Karim, Effects of sugars on the gelation kinetics and texture of duck feet gelatin, Food Hydrocoll. 58 (2016) 267–275, https://doi.org/10.1016/j.foodhyd.2016.02.025.
[28] P. Renato, E. Raccone, S. Costanzo, M. Delmonte, A. Sarrica, R. Pasquino, N. Grizzuti, Gelation kinetics of aqueous gelatin solutions in isothermal conditions via rheological tools, Food Hydrocoll. 111 (2021), 106248, https://doi.org/10.1016/j.foodhyd.2020.106248.
[29] C.M. Bryant, D.J. McClements, Influence of sucrose on NaCl-induced gelation of heat denatured whey protein solutions, Food Res. Int. 33 (2000) 649–653, https://doi.org/10.1016/S0963-9969(00)00109-5.
[30] A. Ishaq, U. ur Rahman, A. Sahar, R. Perveen, A.J. Deering, A.A. Khalil, R.M. Aadil, M.A. Hafeez, A. Khaliq, U. Siddique, Potentiality of analytical approaches to determine gelatin authenticity in food systems: a review, Lwt 121 (2020), 108968, https://doi.org/10.1016/j.lwt.2019.108968.
[31] H.F. Shurvell, 2006 Spectra- structure correlations in the mid- and far-infrared Kingston doi: 10.1002/0470027320.s4101.
[32] A.S. Vaziri, I. Alemzadeh, M. Vossoughi, A.C. Khorasani, Co-microencapsulation of Lactobacillus plantarum and DHA fatty acid in alginate-pectin-gelatin biocomposites, Carbohydr. Polym. 199 (2018) 266–275, https://doi.org/10.1016/j.carbpol.2018.07.002.
[33] Y. Tian, Y. Liu, L. Zhang, Q. Hua, L. Liu, B. Wang, J. Tang, Preparation and characterization of gelatin-sodium alginate/paraffin phase change microcapsules, Colloids Surf. A Physicochem. Eng. Asp. 586 (2020), 124216, https://doi.org/10.1016/j.colsurfa.2019.124216.
[34] F. Liu, B. Sen Chiou, R.J. Avena-Bustillos, Y. Zhang, Y. Li, T.H. McHugh, F. Zhong, Study of combined effects of glycerol and transglutaminase on properties of gelatin films, Food Hydrocoll. 65 (2017) 1–9, https://doi.org/10.1016/j.foodhyd.2016.10.004.
[35] M. Li, B. Li, W. Zhang, Rapid and non-invasive detection and imaging of the hydrocolloid-injected prawns with low-field NMR and MRI, Food Chem. 242 (2018) 16–21, https://doi.org/10.1016/j.foodchem.2017.08.086.
[36] T. Li, X. Rui, W. Li, X. Chen, M. Jiang, M. Dong, Water distribution in tofu and application of T2 relaxation measurements in determination of tofu's water-holding capacity, J. Agric. Food Chem. 62 (2014) 8594–8601, https://doi.org/10.1021/jf503427m.
[37] P. García-Guzmán, L. Medina-Torres, F. Calderas, M.J. Bernad-Bernad, J. Gracia-Mora, B. Mena, O. Manero, Characterization of hybrid microparticles/Montmorillonite composite with raspberry-like morphology for Atorvastatin controlled release, Colloids Surf. B: Biointerfaces 167 (2018) 397–406, https://doi.org/10.1016/j.colsurfb.2018.04.020.
[38] F. Liu, H. Majeed, J. Antoniou, Y. Li, Y. Ma, W. Yokoyama, J. Ma, F. Zhong, Tailoring physical properties of transglutaminase-modi fi ed gelatin films by varying drying temperature, Food Hydrocoll. 58 (2016) 20–28, https://doi.org/10.1016/j.foodhyd.2016.01.026.
[39] B. Giménez, M.P. Montero, Functional and bioactive properties of collagen and gelatin from alternative sources: a review, Food Hydrocoll. 25 (2011) 1813–1827, https://doi.org/10.1016/j.foodhyd.2011.02.007.
[40] C. Peña, K. De, A. Eceiza, R. Ruseckaite, I. Mondragon, Bioresource technology enhancing water repellence and mechanical properties of gelatin films by tannin addition, Bioresour. Technol. 101 (2010) 6836–6842, https://doi.org/10.1016/j.biortech.2010.03.112.
[41] P. Coimbra, M.H. Gil, M. Figueiredo, Tailoring the properties of gelatin films for drug delivery applications: Influence of the chemical cross-linking method, Int. J. Biol. Macromol. 70 (2014) 10–19, https://doi.org/10.1016/j.ijbiomac.2014.06.021.
[42] H. Yang, Y. Wang, Effects of concentration on nanostructural images and physical properties of gelatin from channel catfish skins, Food Hydrocoll. 23 (2009) 577–584, https://doi.org/10.1016/j.foodhyd.2008.04.016.
[43] S. Farris, K.M. Schaich, L.S. Liu, P.H. Cooke, L. Piergiovanni, K.L. Yam, Gelatin-pectin composite films from polyion-complex hydrogels, Food Hydrocoll. 25 (2011) 61–70, https://doi.org/10.1016/j.foodhyd.2010.05.006.